



POLITECNICO
MILANO 1863

RE.PUBLIC@POLIMI

Research Publications at Politecnico di Milano

Post-Print

This is the accepted version of:

L. Dozio

Exact Vibration Solutions for Cross-Ply Laminated Plates with Two Opposite Edges Simply Supported Using Refined Theories of Variable Order

Journal of Sound and Vibration, Vol. 333, N. 8, 2014, p. 2347-2359

doi:10.1016/j.jsv.2013.12.007

The final publication is available at <https://doi.org/10.1016/j.jsv.2013.12.007>

Access to the published version may require subscription.

When citing this work, cite the original published paper.

Permanent link to this version

<http://hdl.handle.net/11311/767075>

Exact vibration solutions for cross-ply laminated plates with two opposite edges simply supported using refined theories of variable order

Lorenzo Dozio

Department of Aerospace Science and Technology, Politecnico di Milano, via La Masa, 34, 20156, Milano, Italy

Abstract

This paper presents exact solutions for free vibration of rectangular cross-ply laminated plates with at least one pair of opposite edges simply supported using refined kinematic theories of variable order. Exact natural frequencies are obtained using an efficient and unified formulation where the solving set of second-order differential equations of motion and related boundary conditions are expressed at layer level in terms of so-called fundamental nuclei having invariant properties with respect to the order of the plate theory. The nuclei are then appropriately expanded according to the number of layers and the order of the theory and the resulting equations are transformed into a first-order model whose solution is obtained by using the state space concept. In this way, the mathematical effort needed to derive analytical solutions is highly reduced. Both higher-order equivalent single-layer and layer-wise theories are considered in this study. Comparisons with other exact solutions are presented and useful benchmark frequency results for symmetric and unsymmetric cross-ply laminates are provided.

Keywords: Free vibration, exact solutions, cross-ply laminated plates, refined theories, higher-order plate theories, layer-wise plate theories.

1. Introduction

Exact vibration analysis of structural elements like beams, plates and shells can be regarded as the theoretical foundation of almost all approximate solution methods. Exact vibration solutions can be relevant for understanding the dynamic response and performing quick parametric and optimization studies. Furthermore, they can serve as a valuable reference for validating numerical methods on their convergence and accuracy and as a basis for developing advanced modelling techniques such as the dynamic stiffness method and the superposition method [1].

By restricting the analysis to plate problems, mathematically exact solutions are typically available as closed-form solutions and series solutions [2]. It is well known that the most common series solution for

Email address: lorenzo.dozio@polimi.it (Lorenzo Dozio)

plates is the so called Navier-type solution. In 1820, Navier introduced a simple method for bending analysis of rectangular plates based on the expansion of the displacement field and the load in a double trigonometric series which identically satisfies the boundary conditions of the problem. Exact results can be obtained for specially orthotropic laminates with all edges simply supported [3]. As in the case of bending, the same double Fourier series can be used for vibration and buckling problems.

It is also well known that exact solutions do exist for rectangular specially orthotropic laminates having one pair of opposite edges simply supported and the remaining two edges having any possible combination of free, simple support or clamped conditions [3]. In this case, the displacement is assumed to be expanded in a single trigonometric series along the direction normal to the pair of opposite simply supported edges. This form of solution is typically referred to as a Lévy-type solution both for static and dynamic problems. However, as stated by Leissa [4], it was first used by Voigt for transverse vibration analysis in 1893, six years before Lévy proposed the same type of solution for solving the plate bending problem.

Exact transverse and in-plane free vibration analysis of isotropic thin plates with at least two opposite edges supported was first provided by Leissa [4] and Gorman [5], respectively. The remarkable work by Hashemi and Arsanjani [6] on moderately thick plates using the Mindlin theory can be considered a counterpart of that undertaken much earlier by Leissa for thin plates. Exact vibration solutions of isotropic multi-span and stepped rectangular plates were presented by Xiang and his co-workers [7, 8, 9, 10]. More recently, Voigt-type solutions for free transverse vibration of thick plates have been also derived via the third-order shear deformation theory [11].

The first-known exact solutions for laminated plates having one pair of opposite simply supported edges are presented in a series of papers by Khdeir, Reddy and Librescu [12, 13, 14, 15, 16, 17]. Assuming a single series solution in one direction, the equations of motion are transformed into a set of ordinary differential equations in the other direction. This set is further transformed into a first-order state space model whose general solution is applied to the boundary conditions to obtain the natural frequencies of the problem. Exact eigenfrequencies of symmetric cross-ply and antisymmetric angle-ply laminated plates are generated using the classical lamination plate theory (CLPT), the first-order shear deformation theory (FSDT) and the third-order shear deformation theory (TSDT) originally proposed by Vlasov for isotropic structures and then extended by Reddy to composite plates and shells [18]. At a later stage, the same method has been applied to plates modelled according to a second-order shear deformation theory [19] and a two-variable refined theory [20].

All the above-cited analytical works are based on two-dimensional (2-D) plate theories essentially built according to a Newtonian approach, where the kinematic variables of the displacement model represent physical quantities like translations, rotations and warping. They neglect plate thickness stretching and are simple enough to yield economical models that could be handled rather easily by analytical techniques. However, they may introduce overly simplified assumptions concerning the three-dimensional (3-D) kine-

matics of deformation of the plate. Indeed, multilayered constructions are typically characterized by high transverse shear and normal deformation and by a displacement field with discontinuous derivatives along the thickness direction (so called *zig-zag* effect). Such complicating effects are completely discarded or only approximately captured by FSDT and TSDT. The accuracy of Newtonian-based plate theories in predicting the laminate vibration behavior is even worse when the thickness-to-length ratio of the plate increases and the frequency range of interest widens.

Owing to the complex nature of the 3-D deformation of laminated plates, many refinements of FSDT have been proposed in the literature to improve the accuracy of 2-D plate models without resorting to a cumbersome fully 3-D analysis. They are typically referred to as refined or higher-order shear deformation theories [21, 22, 23, 24, 25, 26] and belong to the class of theories developed according to a Lagrangian approach, where each kinematic variable of the assumed displacement model can be considered as a generalized coordinate without a direct physical meaning. Generally speaking, Lagrangian-based plate theories can be classified as equivalent single-layer (ESL) models, where the classical FSDT displacement form is enriched with higher-order terms as series expansion of the thickness coordinate, and layer-wise (LW) models, in which a different displacement field is postulated in each layer and appropriate continuity conditions are enforced at each layer interface. The number of expansion terms for each displacement variable included into the plate model is referred to as the order of the theory.

The disadvantage of refined plate theories is the complexity of the resulting models, which are lengthy and tedious to derive and difficult to solve by analytical methods. To the best author's knowledge, exact Voigt-type solutions based on a refined theory have been obtained only recently by Boscolo [27]. In this work, free vibration of rectangular laminated plates is solved using a first-order layer-wise theory. Exact eigenfrequencies are validated by comparison with available analytical 3-D and 2-D Navier-type solutions. The approach developed in Ref. [27] is used by Boscolo and Banerjee [28] within the framework of the dynamic stiffness method. Although the first-order layer-wise displacement model may suffer from some limitations in terms of accuracy and efficacy, the effort is remarkable.

The aim of the present work is to present an efficient, unified and somehow automatic method to provide exact vibration solutions of thin and thick cross-ply laminates with at least two opposite edges simply supported. It can be considered as a generalization of what presented in Ref. [27]. The novel procedure introduced here overcomes the shortcomings of the previous formulations which were limited to plate models derived from a single theory with fixed kinematics (i.e., fixed order). Using the present approach, the solving equations must not be re-derived when a different order of the theory is adopted and thus the mathematical effort needed to obtain analytical solutions is substantially reduced. In particular, both two-dimensional ESL and LW theories of variable order are considered. As a result, a considerable number of new exact frequency results are obtained which can be useful as benchmark solutions for future comparison.

2. Governing equations at layer level

2.1. Preliminaries

Consider an unloaded cross-ply laminated rectangular plate of length a , width b and thickness h (see Figure 1). The plate consists of N_ℓ layers, which are assumed to be homogeneous and made of orthotropic material of mass density ρ^k . The k th layer has thickness h_k and is located between interfaces $z = z_k$ and $z = z_{k+1}$ in the thickness direction. The layer numbering begins at the bottom surface of the laminate (i.e., $z_1 = -h/2$).

The equations of motion are derived from the principle of virtual displacements (PVD), which is written as follows

$$\sum_{k=1}^{N_\ell} \int_{\Omega} \int_{z_k}^{z_{k+1}} \left(\delta \boldsymbol{\epsilon}_p^k \mathbf{\sigma}_p^k + \delta \boldsymbol{\epsilon}_n^k \mathbf{\sigma}_n^k \right) d\zeta d\Omega = - \sum_{k=1}^{N_\ell} \int_{\Omega} \int_{z_k}^{z_{k+1}} \delta \mathbf{u}^k \rho^k \frac{\partial^2 \mathbf{u}^k}{\partial t^2} d\zeta d\Omega \quad (1)$$

where

$$\mathbf{u}^k(x, y, \zeta_k, t) = \left[u^k(x, y, \zeta_k, t) \quad v^k(x, y, \zeta_k, t) \quad w^k(x, y, \zeta_k, t) \right]^T \quad (2)$$

is the displacement vector at any point of the layer k , ζ_k is the local dimensionless thickness coordinate ($-1 \leq \zeta_k \leq +1$), $\Omega = [0, a] \times [0, b]$, and the stress and strain vectors for the k th layer are partitioned into in-plane and out-of-plane (normal) components as follows

$$\begin{aligned} \boldsymbol{\sigma}_p^k &= \left[\sigma_{xx}^k \quad \sigma_{yy}^k \quad \tau_{xy}^k \right]^T, & \boldsymbol{\epsilon}_p^k &= \left[\epsilon_{xx}^k \quad \epsilon_{yy}^k \quad \gamma_{xy}^k \right]^T \\ \boldsymbol{\sigma}_n^k &= \left[\tau_{xz}^k \quad \tau_{yz}^k \quad \sigma_{zz}^k \right]^T, & \boldsymbol{\epsilon}_n^k &= \left[\gamma_{xz}^k \quad \gamma_{yz}^k \quad \epsilon_{zz}^k \right]^T \end{aligned}$$

The linear strain-displacements relations are expressed in matrix notation as

$$\boldsymbol{\epsilon}_p^k = \mathcal{D}_p \mathbf{u}^k, \quad \boldsymbol{\epsilon}_n^k = \mathcal{D}_n \mathbf{u}^k + \frac{\partial}{\partial z} \mathbf{u}^k \quad (3)$$

where

$$\mathcal{D}_p = \begin{bmatrix} \partial/\partial x & 0 & 0 \\ 0 & \partial/\partial y & 0 \\ \partial/\partial y & \partial/\partial x & 0 \end{bmatrix}, \quad \mathcal{D}_n = \begin{bmatrix} 0 & 0 & \partial/\partial z \\ 0 & 0 & \partial/\partial z \\ 0 & 0 & 0 \end{bmatrix}$$

2.2. Refined theories of variable order

According to the technique proposed by Carrera [29], an entire class of 2-D refined LW plate theories are employed by expressing the displacement vector \mathbf{u}^k through the Einstein notation as follows

$$\mathbf{u}^k(x, y, \zeta_k, t) = F_\tau(\zeta_k) \mathbf{u}_\tau^k(x, y, t) \quad (4)$$

where τ is the theory-related index, $F_\tau(\zeta_k)$ are appropriate thickness functions defined locally for the layer, and

$$\mathbf{u}_\tau^k(x, y, t) = \left[u_\tau^k(x, y, t) \quad v_\tau^k(x, y, t) \quad w_\tau^k(x, y, t) \right]^T \quad (5)$$

is the vector of generalized (Lagrangian) kinematic coordinates in the assumed displacement model corresponding to index τ . Various theories of different order can be obtained by choosing the type of thickness functions and the range values of τ . In this work, a family of layer-wise theories of variable order N , which is a free parameter of the formulation, is considered by assuming $\tau = t, b, r$ ($r = 2, \dots, N$) and selecting

$$F_t(\zeta_k) = \frac{1 + \zeta_k}{2}; \quad F_b(\zeta_k) = \frac{1 - \zeta_k}{2}; \quad F_r(\zeta_k) = P_r(\zeta_k) - P_{r-2}(\zeta_k) \quad (6)$$

where $P_i(\zeta_k)$ is the Legendre polynomial of i th order. In so doing, the displacement variables \mathbf{u}_b^k and \mathbf{u}_t^k are the actual values at the bottom and top surfaces of layer k , respectively, and the interlaminar displacement continuity can be easily imposed as $\mathbf{u}_t^k = \mathbf{u}_b^{k+1}$ for $k = 1, 2, \dots, N_\ell - 1$. Each member of the family is shortly denoted here by the acronym LDN, which stands for (L)ayer-wise (D)isplacement-based theory of order N . Note that the number of degrees of freedom for a LDN theory is given by $3(N + 1)N_\ell - 3(N_\ell - 1)$.

The same formal approach can be also used to define a class of ESL plate theories. Since in this case the kinematics is layer-independent, the k index in Eq. (4) is dropped and global thickness functions F_τ are selected. The classical z expansion is here adopted in terms of Taylor polynomials by assuming

$$F_\tau = z^\tau \quad (7)$$

where now $t = 0$ and $b = 1$. The related N -order ESL theory is denoted by the acronym EDN, which stands for (E)quivalent single-layer (D)isplacement-based theory of order N . As such, the number of degrees of freedom for a EDN theory is $3(N + 1)$. It is noted that, according to the present framework, a first-order and third-order ESL theory are defined, respectively, as follows:

$$\text{ED1 (first-order ESL theory):} \quad \begin{cases} u = u_0 + zu_1 \\ v = v_0 + zv_1 \\ w = w_0 + zw_1 \end{cases} \quad (8)$$

$$\text{ED3 (third-order ESL theory):} \quad \begin{cases} u = u_0 + zu_1 + z^2u_2 + z^3u_3 \\ v = v_0 + zv_1 + z^2v_2 + z^3v_3 \\ w = w_0 + zw_1 + z^2w_2 + z^3w_3 \end{cases} \quad (9)$$

Therefore, they differ from conventional FSDT and TSDT. In particular, ED1 includes a first-order term in the expansion of the transverse displacement w , which is not present in FSDT. ED3 model contains 12 kinematic variables compared to 5 of TSDT since transverse normal strain effects are included through the third-order expansion of w and no specific conditions (such as traction-free boundary conditions on the top and bottom faces of the laminate) are imposed to reduce the number of dependent unknowns. As discussed in Dozio and Carrera [30], classical FSDT can be recovered from ED1 model after imposing the condition of null transverse normal stresses and introducing an appropriate shear correction factor into the constitutive equations. Note also that ED1 exhibits a thickness locking problem [31], which appears since it

shows a constant distribution of transverse normal strain. Therefore, it should not be used as is, especially if relatively thin plates are considered. In order to avoid thickness locking, ED1 can be reduced to FSĐT as explained before.

2.3. Equations in terms of stress resultants

Substituting Eq. (4) into the strain-displacement relations (3) and the PVD statement yields

$$\sum_{k=1}^{N_\ell} \int_{\Omega} \left[(\mathcal{D}_p \delta \mathbf{u}_\tau^k)^T \mathcal{R}_{p\tau}^k + (\mathcal{D}_n \delta \mathbf{u}_\tau^k)^T \mathcal{R}_{n\tau}^k + \delta \mathbf{u}_\tau^k{}^T \mathcal{R}_{n\tau z}^k \right] d\Omega = - \sum_{k=1}^{N_\ell} \int_{\Omega} \delta \mathbf{u}_\tau^k{}^T \rho^k J_{\tau s}^k \frac{\partial^2 \mathbf{u}_s^k}{\partial t^2} d\Omega \quad (10)$$

where the index s has the same meaning of τ , $J_{\tau s}^k$ is a thickness integrals defined as

$$J_{\tau s}^k = \int_{z_k}^{z_{k+1}} F_\tau F_s d\zeta \quad (11)$$

and the following stress resultants are introduced

$$\mathcal{R}_{p\tau}^k = \begin{Bmatrix} \mathcal{R}_{xx\tau}^k \\ \mathcal{R}_{yy\tau}^k \\ \mathcal{R}_{xy\tau}^k \end{Bmatrix} = \int_{z_k}^{z_{k+1}} F_\tau \boldsymbol{\sigma}_p^k d\zeta, \quad \mathcal{R}_{n\tau}^k = \begin{Bmatrix} \mathcal{R}_{xz\tau}^k \\ \mathcal{R}_{yz\tau}^k \\ \mathcal{R}_{zz\tau}^k \end{Bmatrix} = \int_{z_k}^{z_{k+1}} F_\tau \boldsymbol{\sigma}_n^k d\zeta, \quad \mathcal{R}_{n\tau z}^k = \int_{z_k}^{z_{k+1}} F_{\tau z} \boldsymbol{\sigma}_n^k d\zeta \quad (12)$$

in which $F_{\tau z} = dF_\tau/dz$.

After integrating by parts Eq. (10) and exploiting the arbitrariness of $\delta \mathbf{u}_\tau^k$ over the plate domain Ω , the equations of motion can be written in terms of stress resultants for any layer k as

$$\mathcal{D}_p^T \mathcal{R}_{p\tau}^k + \mathcal{D}_n^T \mathcal{R}_{n\tau}^k - \mathcal{R}_{n\tau z}^k = \rho^k J_{\tau s}^k \frac{\partial^2 \mathbf{u}_s^k}{\partial t^2} \quad (13)$$

From the boundary terms, the following conditions along each plate edge are obtained

$$\begin{aligned} u_\tau^k = 0 \quad \text{or} \quad n_x \mathcal{R}_{xx\tau}^k + n_y \mathcal{R}_{xy\tau}^k &= 0 \\ v_\tau^k = 0 \quad \text{or} \quad n_y \mathcal{R}_{yy\tau}^k + n_x \mathcal{R}_{xy\tau}^k &= 0 \\ w_\tau^k = 0 \quad \text{or} \quad n_x \mathcal{R}_{xz\tau}^k + n_y \mathcal{R}_{yz\tau}^k &= 0 \end{aligned} \quad (14)$$

where n_x and n_y are the components of the outward normal to the edge.

2.4. Equations in terms of displacements

Assuming a linearly elastic material, the constitutive equation in the laminate reference coordinate system are written as

$$\begin{aligned} \boldsymbol{\sigma}_p^k &= \tilde{\mathbf{C}}_{pp}^k \boldsymbol{\epsilon}_p^k + \tilde{\mathbf{C}}_{pn}^k \boldsymbol{\epsilon}_n^k \\ \boldsymbol{\sigma}_n^k &= \tilde{\mathbf{C}}_{pn}^{kT} \boldsymbol{\epsilon}_p^k + \tilde{\mathbf{C}}_{nn}^k \boldsymbol{\epsilon}_n^k \end{aligned} \quad (15)$$

where the matrices of stiffness coefficients for the k th layer of a cross-ply laminate are given by

$$\tilde{\mathbf{C}}_{\text{pp}}^k = \begin{bmatrix} \tilde{C}_{11}^k & \tilde{C}_{12}^k & 0 \\ \tilde{C}_{12}^k & \tilde{C}_{22}^k & 0 \\ 0 & 0 & \tilde{C}_{66}^k \end{bmatrix}, \quad \tilde{\mathbf{C}}_{\text{pn}}^k = \begin{bmatrix} 0 & 0 & \tilde{C}_{13}^k \\ 0 & 0 & \tilde{C}_{23}^k \\ 0 & 0 & 0 \end{bmatrix}, \quad \tilde{\mathbf{C}}_{\text{nn}}^k = \begin{bmatrix} \tilde{C}_{55}^k & 0 & 0 \\ 0 & \tilde{C}_{44}^k & 0 \\ 0 & 0 & \tilde{C}_{33}^k \end{bmatrix} \quad (16)$$

Note that the stiffness constants \tilde{C}_{ij}^k are derived from the stiffness coefficients C_{ij}^k expressed in the layer reference system through a proper coordinate transformation [3].

By inserting Eq. (15) into Eq. (12) and using again the strain-displacement relations, the equations of motion at layer level expressed in Eq. (13) can be compactly written in terms of displacement coordinates as follows

$$\mathcal{L}^{k\tau s} \mathbf{u}_s^k = \rho^k J_{\tau s}^k \frac{\partial^2 \mathbf{u}_s^k}{\partial t^2} \quad (17)$$

where $\mathcal{L}^{k\tau s}$ is a 3×3 matrix of differential operators called *fundamental nucleus* of the formulation given by

$$\begin{aligned} \mathcal{L}^{k\tau s} &= \mathcal{D}_{\text{p}}^{\text{T}} \tilde{\mathbf{C}}_{\text{pp}}^k J_{\tau s}^k \mathcal{D}_{\text{p}} + \mathcal{D}_{\text{p}}^{\text{T}} \tilde{\mathbf{C}}_{\text{pn}}^k J_{\tau s}^k \mathcal{D}_{\text{n}} + \mathcal{D}_{\text{p}}^{\text{T}} \tilde{\mathbf{C}}_{\text{pn}}^k J_{\tau s_z}^k \\ &+ \mathcal{D}_{\text{n}}^{\text{T}} \tilde{\mathbf{C}}_{\text{pn}}^k J_{\tau s}^k \mathcal{D}_{\text{p}} + \mathcal{D}_{\text{n}}^{\text{T}} \tilde{\mathbf{C}}_{\text{nn}}^k J_{\tau s}^k \mathcal{D}_{\text{n}} + \mathcal{D}_{\text{n}}^{\text{T}} \tilde{\mathbf{C}}_{\text{nn}}^k J_{\tau s_z}^k \\ &- \tilde{\mathbf{C}}_{\text{pn}}^k J_{\tau s_z}^k \mathcal{D}_{\text{p}} - \tilde{\mathbf{C}}_{\text{nn}}^k J_{\tau s_z}^k \mathcal{D}_{\text{n}} - \tilde{\mathbf{C}}_{\text{nn}}^k J_{\tau s_z}^k \end{aligned} \quad (18)$$

and

$$J_{\tau s_z}^k = \int_{z_k}^{z_{k+1}} F_{\tau} F_{s_z} d\zeta, \quad J_{\tau z s}^k = \int_{z_k}^{z_{k+1}} F_{\tau z} F_s d\zeta, \quad J_{\tau z s_z}^k = \int_{z_k}^{z_{k+1}} F_{\tau z} F_{s_z} d\zeta \quad (19)$$

are thickness integrals.

Accordingly, the boundary conditions in Eq. (14) can be compactly written for each edge of the plate as

$$\mathcal{B}^{k\tau s} \mathbf{u}_s^k = \mathbf{0} \quad (20)$$

where $\mathcal{B}^{k\tau s}$ is a 3×3 fundamental nucleus matrix of boundary-related differential operators.

3. The solution procedure

3.1. Voigt-type solution

Let's now assume that the plate is simply-supported at edges $y = 0$ and $y = b$ and the remaining edges $x = 0$ and $x = a$ can have any combination of free, simply-supported or clamped condition. According to the outlined framework, the condition of simple support at $y = 0, b$ is specified herein for any theory-related index s as follows

$$\begin{aligned} u_s^k &= 0 \\ \mathcal{R}_{yy_s}^k &= 0 \quad (y = 0, b) \\ w_s^k &= 0 \end{aligned} \quad (21)$$

A solution for free harmonic motion of the laminate which satisfies the above boundary conditions is sought as follows

$$\mathbf{u}_s^k = \left\{ \begin{array}{l} U_{sm}^k(x) \sin(\beta_m y) \\ V_{sm}^k(x) \cos(\beta_m y) \\ W_{sm}^k(x) \sin(\beta_m y) \end{array} \right\} e^{j\omega_m t} \quad (m = 1, 2, \dots) \quad (22)$$

where ω_m denotes the unknown eigenfrequency associated with the m -th eigenmode and $\beta_m = m\pi/b$. Note that the expression in Eq. (22) is indeed a series solution with respect to index m due to the same Einstein notation used before for theory-related indices.

3.2. Ordinary differential equations and fundamental nuclei of the solution

Substituting the solution (22) into Eqs. (17) yields, for each $m = 1, 2, \dots$, the following system of second-order ordinary differential equations for the k th layer

$$\mathbf{L}_2^{k\tau s} \frac{d^2 \mathbf{U}_s^k}{dx^2} - \mathbf{L}_1^{k\tau s} \frac{d \mathbf{U}_s^k}{dx} - \mathbf{L}_0^{k\tau s} \mathbf{U}_s^k = \mathbf{0} \quad (23)$$

where

$$\mathbf{U}_s^k(x) = \left[U_{sm}^k(x) \quad V_{sm}^k(x) \quad W_{sm}^k(x) \right]^T \quad (24)$$

is the vector of unknown amplitudes and

$$\mathbf{L}_2^{k\tau s} = J_{\tau s}^k \begin{bmatrix} \tilde{C}_{11}^k & 0 & 0 \\ 0 & \tilde{C}_{66}^k & 0 \\ 0 & 0 & \tilde{C}_{55}^k \end{bmatrix} \quad (25)$$

$$\mathbf{L}_1^{k\tau s} = \begin{bmatrix} 0 & l_{12} & l_{13} \\ -l_{12} & 0 & 0 \\ -l_{13} & 0 & 0 \end{bmatrix}, \quad \begin{array}{l} l_{12} = \beta_m (\tilde{C}_{12}^k + \tilde{C}_{66}^k) J_{\tau s}^k \\ l_{13} = \tilde{C}_{55}^k J_{\tau_z s}^k - \tilde{C}_{13}^k J_{\tau s_z}^k \end{array} \quad (26)$$

$$\mathbf{L}_0^{k\tau s} = \begin{bmatrix} l_{11} & 0 & 0 \\ 0 & l_{22} & l_{23} \\ 0 & l_{23} & l_{33} \end{bmatrix} \quad \begin{array}{l} l_{11} = \beta_m^2 \tilde{C}_{66}^k J_{\tau s}^k + \tilde{C}_{55}^k J_{\tau_z s_z}^k - \rho^k J_{\tau s}^k \omega_m^2 \\ l_{22} = \beta_m^2 \tilde{C}_{22}^k J_{\tau s}^k + \tilde{C}_{44}^k J_{\tau_z s_z}^k - \rho^k J_{\tau s}^k \omega_m^2 \\ l_{33} = \beta_m^2 \tilde{C}_{44}^k J_{\tau s}^k + \tilde{C}_{33}^k J_{\tau_z s_z}^k - \rho^k J_{\tau s}^k \omega_m^2 \\ l_{23} = \beta_m (\tilde{C}_{44}^k J_{\tau_z s}^k - \tilde{C}_{23}^k J_{\tau s_z}^k) \end{array} \quad (27)$$

are the 3×3 matrices representing the fundamental nuclei of the governing equations along x direction.

Doing the same for the boundary conditions at edges $x = 0$ and $x = a$, the following equations for layer k are obtained

$$\mathbf{B}_1^{k\tau s} \frac{d \mathbf{U}_s^k}{dx} + \mathbf{B}_0^{k\tau s} \mathbf{U}_s^k = \mathbf{0} \quad (x = 0, a) \quad (28)$$

where $\mathbf{B}_i^{k\tau s}$ ($i = 0, 1$) is the 3×3 fundamental nucleus corresponding to the boundary conditions. According to the type of edge condition at $x = 0, a$, the boundary-related nuclei are expressed as follows

- clamped edge:

$$\mathbf{B}_1^{k\tau s} = \mathbf{0}, \quad \mathbf{B}_0^{k\tau s} = \mathbf{I} \quad (29)$$

- free edge:

$$\mathbf{B}_1^{k\tau s} = J_{\tau s}^k \begin{bmatrix} \tilde{C}_{11}^k & 0 & 0 \\ 0 & \tilde{C}_{66}^k & 0 \\ 0 & 0 & \tilde{C}_{55}^k \end{bmatrix}, \quad \mathbf{B}_0^{k\tau s} = \begin{bmatrix} 0 & -\beta_m \tilde{C}_{12}^k J_{\tau s}^k & \tilde{C}_{13}^k J_{\tau s_z}^k \\ \beta_m \tilde{C}_{66}^k J_{\tau s}^k & 0 & 0 \\ \tilde{C}_{55}^k J_{\tau s_z}^k & 0 & 0 \end{bmatrix} \quad (30)$$

- simply-supported edge:

$$\mathbf{B}_1^{k\tau s} = J_{\tau s}^k \begin{bmatrix} \tilde{C}_{11}^k & 0 & 0 \\ 0 & 0 & 0 \\ 0 & 0 & 0 \end{bmatrix}, \quad \mathbf{B}_0^{k\tau s} = \begin{bmatrix} 0 & -\beta_m \tilde{C}_{12}^k J_{\tau s}^k & \tilde{C}_{13}^k J_{\tau s_z}^k \\ 0 & 0 & 0 \\ 0 & 0 & 0 \end{bmatrix} \quad (31)$$

3.3. Equations of the multilayered plate

Equations (23) and (28) are written at layer level in terms of fundamental nuclei $\mathbf{L}_i^{k\tau s}$ and $\mathbf{B}_i^{k\tau s}$. In order to obtain the governing equations and related boundary conditions of the multilayered plate according to the assumed kinematic theory, a simple expansion and assembly-like procedure is applied. The procedure is graphically depicted in Figure 2 for \mathbf{L} matrices.

First, by varying the theory-related indices τ and s over the defined ranges, the nuclei $\mathbf{L}_i^{k\tau s}$ and $\mathbf{B}_i^{k\tau s}$ are expanded (see Figure 2a) so that a new system of equations and related boundary conditions is obtained as follows

$$\begin{aligned} \mathbf{L}_2^k \frac{d^2 \mathbf{U}^k}{dx^2} - \mathbf{L}_1^k \frac{d\mathbf{U}^k}{dx} - \mathbf{L}_0^k \mathbf{U}^k &= \mathbf{0} \\ \mathbf{B}_1^k \frac{d\mathbf{U}^k}{dx} + \mathbf{B}_0^k \mathbf{U}^k &= \mathbf{0} \quad (x = 0, a) \end{aligned} \quad (32)$$

where

$$\mathbf{U}^k(x) = \begin{bmatrix} \mathbf{U}_t^{k\tau} (x) & \mathbf{U}_r^{k\tau} (x) & \mathbf{U}_b^{k\tau} (x) \end{bmatrix}^T \quad (33)$$

and

$$\mathbf{L}_i^k = \begin{bmatrix} \mathbf{L}_i^{ktt} & \mathbf{L}_i^{ktr} & \mathbf{L}_i^{ktb} \\ \mathbf{L}_i^{krt} & \mathbf{L}_i^{krr} & \mathbf{L}_i^{krb} \\ \mathbf{L}_i^{kbt} & \mathbf{L}_i^{kbr} & \mathbf{L}_i^{kbb} \end{bmatrix}, \quad \mathbf{B}_i^k = \begin{bmatrix} \mathbf{B}_i^{ktt} & \mathbf{B}_i^{ktr} & \mathbf{B}_i^{ktb} \\ \mathbf{B}_i^{krt} & \mathbf{B}_i^{krr} & \mathbf{B}_i^{krb} \\ \mathbf{B}_i^{kbt} & \mathbf{B}_i^{kbr} & \mathbf{B}_i^{kbb} \end{bmatrix} \quad (34)$$

Note that \mathbf{L}_i^k and \mathbf{B}_i^k are square matrices of dimension $3(N+1)$.

Then, the final set of equations is written as

$$\begin{aligned} \mathbf{L}_2 \frac{d^2 \mathbf{U}}{dx^2} - \mathbf{L}_1 \frac{d\mathbf{U}}{dx} - \mathbf{L}_0 \mathbf{U} &= \mathbf{0} \\ \mathbf{B}_1 \frac{d\mathbf{U}}{dx} + \mathbf{B}_0 \mathbf{U} &= \mathbf{0} \quad (x = 0, a) \end{aligned} \quad (35)$$

where $\mathbf{U}(x)$ is the vector containing all the independent kinematic variables $\mathbf{U}^k(x)$ ($k = 1, \dots, N_\ell$), and the resulting matrices \mathbf{L}_i and \mathbf{B}_i are simply summed layer-by-layer in case of ESL theories or assembled by enforcing the interlaminar continuity condition in case of LW theories (see Figure 2b).

3.4. State-space model and solution

A state space approach is used to solve the free vibration problem by converting Eqs. (35) into a first-order form as follows

$$\begin{aligned} \frac{d\mathbf{Z}}{dx} &= \mathbf{A}\mathbf{Z} \\ \mathbf{B}\mathbf{Z} &= \mathbf{0} \quad (x = 0, a) \end{aligned} \quad (36)$$

where

$$\mathbf{Z}(x) = \begin{Bmatrix} d\mathbf{U}/dx \\ \mathbf{U} \end{Bmatrix} \quad (37)$$

and

$$\mathbf{A} = \begin{bmatrix} \mathbf{L}_2 & \mathbf{0} \\ \mathbf{0} & \mathbf{I} \end{bmatrix}^{-1} \begin{bmatrix} \mathbf{L}_1 & \mathbf{L}_0 \\ \mathbf{I} & \mathbf{0} \end{bmatrix}, \quad \mathbf{B} = \begin{bmatrix} \mathbf{B}_1 & \mathbf{B}_0 \end{bmatrix} \quad (38)$$

A general solution can be expressed as

$$\mathbf{Z}(x) = e^{\mathbf{A}x} \mathbf{c} \quad (39)$$

where \mathbf{c} is a vector of constants connected to boundary conditions. Using a spectral decomposition of the exponential matrix, the solution can be written as

$$\mathbf{Z}(x) = \mathbf{V}\text{Diag}(e^{\lambda_i x}) \mathbf{V}^{-1} \mathbf{c} \quad (40)$$

where \mathbf{V} is the matrix of eigenvectors of \mathbf{A} and λ_i are the corresponding eigenvalues. Replacement of solution (40) into the system of boundary equations in Eq. (36) yields a homogeneous system

$$\mathbf{B}\mathbf{V}\text{Diag}(e^{\lambda_i x}) \mathbf{V}^{-1} \mathbf{c} = \mathbf{H}\mathbf{c} = \mathbf{0} \quad (x = 0, a) \quad (41)$$

The natural frequencies associated with the m -th mode are determined by setting $|\mathbf{H}| = 0$. Note that, since $\mathbf{H} = \mathbf{H}(\omega_m)$, an iterative numerical procedure must be employed to derive the frequency parameters.

3.5. Summary of the method

As a summary, the present method can be implemented through the following steps:

1. Select the number of half waves m of the vibration mode in the y direction.
2. Build the fundamental nuclei $\mathbf{B}_i^{k\tau s}$ ($i = 0, 1$) using Eqs. (29-31) according to the edge condition at $x = 0$ and $x = a$.

3. Expand the nuclei $\mathbf{B}_i^{k\tau s}$ as outlined in Figure 2 in order to build \mathbf{B}_i matrices and the related \mathbf{B} matrix in Eq. (38).
4. For any iteration step over the selected range values of ω_m :
 - (a) Build the fundamental nuclei $\mathbf{L}_i^{k\tau s}$ ($i = 0, 1, 2$).
 - (b) Expand the nuclei $\mathbf{L}_i^{k\tau s}$ as outlined in Figure 2 in order to build \mathbf{L}_i matrices and compute \mathbf{A} matrix in Eq. (38).
 - (c) Compute the spectral decomposition of matrix \mathbf{A} .
 - (d) Compute the \mathbf{H} matrix in Eq. (41) and its determinant.
 - (e) Check if the determinant changes sign. If yes, the value of the natural frequency is found by using the bisection method.

4. Numerical results

4.1. Validation of the method

The present method is first validated by comparison with Navier-type solutions and 3-D exact eigenfrequencies for a square fully simply-supported $[0^\circ/90^\circ/0^\circ/90^\circ]$ plate having side-to-thickness ratio $b/h = 10$. The four layers are assumed to have identical thickness and to be made of an orthotropic material with the following properties: $E_1 = 25.1 \times 10^6$ psi, $E_2 = 4.8 \times 10^6$ psi, $E_3 = 0.75 \times 10^6$ psi, $G_{12} = 1.36 \times 10^6$ psi, $G_{13} = 1.2 \times 10^6$ psi, $G_{23} = 0.47 \times 10^6$ psi, $\nu_{12} = 0.036$, $\nu_{13} = 0.25$, $\nu_{23} = 0.171$. Table 1 shows the first five non-dimensional natural frequencies $\Omega = \omega h \sqrt{\rho/E_2}$ corresponding to two vibration mode combinations $(l, m) = (1, 1)$ and $(2, 1)$, where l is the number of half waves in the x direction. Frequency solutions computed by the present method using higher-order ESL and LW theories up to order $N = 4$ are shown along with Navier-type solutions based on the same set of refined plate theories and 3-D exact results from Ref. [32].

It can be observed that the present exact solutions are perfectly identical to the exact Navier-type ones. The degree of accuracy of 2-D ESL theories with respect to 3-D analysis improves by increasing the order N of the theory since the higher-order terms included into the assumed kinematic field help in reproducing the correct mechanical behavior of the plate. The same is true for the class of LW theories considered herein. It is also shown that, as expected, present exact 2-D frequency values are always higher than the ones computed by the 3-D exact model. Note that, in general, LW theories of order N provide more accurate results than ESL theories of the same order due to the richer displacement model of a layerwise description and the capability of predicting the through-the-thickness zig-zag behavior of the displacements in correspondence of each layer interface. Moreover, the discrepancy between ESL theories and the 3-D model increases when higher-order vibration modes are considered. As a final remark, excellent agreement with 3-D results is observed when LD3 and LD4 theories are adopted.

4.2. Comparison with CLPT and TSDT

Some examples corresponding to a three-layer symmetric $[0^\circ/90^\circ/0^\circ]$ square laminated plate for which exact vibration solutions are available in the literature are now analyzed. For the sake of comparison, the following dimensionless properties of a fiber-reinforced material are used: $E_1/E_2 = 40$, $E_2 = E_3$, $G_{12}/E_2 = G_{13}/E_2 = 0.6$, $G_{23}/E_2 = 0.5$, $\nu_{12} = \nu_{13} = \nu_{23} = 0.25$. Six different combinations of boundary conditions are considered (see Figure 3). The combination of simply-supported (S), free (F) and clamped (C) edges is denoted by a two-letter compact notation corresponding to the conditions at edge $x = 0$ and $x = a$, respectively.

First, exact dimensionless fundamental frequency $\Omega = (\omega b^2/h)\sqrt{\rho/E_2}$ is shown in Table 2 for various length-to-thickness ratios b/h corresponding to thin, moderately thick and thick plates. Present solutions computed with ED3 and LD4 theory are compared with those obtained by Hadian and Nayfeh [33] with the third-order shear deformation theory (TSDT). The values of the classical lamination plate theory (CLPT) are also presented as a reference. ED3 and LD4 are selected as representative models of higher-order shear and normal deformation theories and very refined quasi 3-D approaches, respectively. It is shown in all cases that, as the thickness-to-length ratio increases, the fundamental frequency decreases at a rate which depends on the boundary conditions. It is also observed that, as expected, the frequency results are all in good agreement when $b/h = 50$ and the error of CLPT increases dramatically when the plate gets thicker. The discrepancy between TDST and ED3 is negligible for moderately thick plates ($b/h = 20$ and 10) having any combination of boundary conditions. However, rather inaccurate results are obtained using TSDT when SC and CC thick plates with $b/h = 5$ are considered. Note also that, by comparing results of ED3 and LD4 theories, the fundamental frequency is well estimated by a third-order ESL theory without the need of relying to a more costly layer-wise approach.

The next numerical study deals with the effect of the in-plane orthotropy ratio E_1/E_2 on the fundamental frequency of the cross-ply plate considered before. Exact dimensionless frequency $\Omega = (\omega b^2/h)\sqrt{\rho/E_2}$ is shown in Table 3 for a moderately thick plate with $b/h = 10$ and various E_1/E_2 ratios ranging from 2 to 30. As before, present solutions are reported only for ED3 and LD4 theory. When available, they are compared with those obtained by Khdeir [17] using TSDT and CLPT. An excellent agreement between TSDT and more refined kinematic theories is observed for low ($E_1/E_2 = 2$) to moderate ($E_1/E_2 = 20$) orthotropy ratios and for all combinations of boundary conditions. The exact fundamental frequency is slightly overestimated by TSDT when E_1/E_2 is high, especially when edges $x = 0$ and $x = a$ are clamped.

4.3. Higher-order modes

The effectiveness of refined 2-D ESL and LW theories in providing highly accurate eigenfrequencies can be appreciated when higher-order vibration modes are evaluated. For this purpose, the fundamental frequency $\Omega = (\omega b^2/h)\sqrt{\rho/E_2}$ of a $[0^\circ/90^\circ/0^\circ]$ plate with $a = b$ and $b/h = 10$ is computed for increasing values

of number m of half waves in the y direction. Each layer of the laminate has the following dimensionless material properties: $E_1/E_2 = 40$, $E_2 = E_3$, $G_{12}/E_2 = G_{13}/E_2 = 0.6$, $G_{23}/E_2 = 0.5$, $\nu_{12} = \nu_{13} = \nu_{23} = 0.25$. The frequency results are presented in Table 4 up to $m = 5$ for two representative ESL theories (ED3 and ED4) and LW theories (LD1 and LD4). Comparison values computed using TSDT [17] and a semi-analytical 3-D approach [34] are also reported for $m = 1, 2, 3$. 3-D reference results from Chen and Lue [34] are only available for SS, SC, CC and FC boundary conditions.

It is seen that LD4 is capable of providing values very close to 3-D frequencies even if high values of m are considered. The accuracy of ESL theories and TSDT is comparable and acceptable when $m = 1$ and $m = 2$, but the difference with respect to 3-D analysis is quite considerable at higher m values. A first-order layer-wise theory may provide better results than ESL approaches. However, it is observed that accurate prediction of the natural frequency of higher-order modes requires refined (i.e., higher-order) layer-wise approaches. Results computed using LD4 for $m = 4$ and $m = 5$ are considered to be reliable exact benchmark values for future comparison. Finally, note that eigensolutions of high-frequency modes tend to the same value, as expected, irrespective of the boundary conditions of the problem.

5. Conclusions

A powerful and efficient formulation capable of providing exact Voigt-type solutions for cross-ply rectangular laminates using refined equivalent single-layer and layer-wise 2-D theories of variable order is presented. The novelty and main advantage of the approach is its invariance with respect to the assumed plate kinematics, so that the mathematical effort required to derive and obtain the analytical solutions is order-independent. Several first-known exact frequency values are obtained for thin, moderately thick and thick plates with at least one pair of opposite edges simply supported. The present method is validated against Navier-type solutions and 3-D exact analysis. Comparisons with classical plate theories and discussion on their accuracy are also provided as a function of the plate thickness ratio, in-plane orthotropicity ratio and evaluation of higher-order modes.

References

- [1] D.J. Gorman, *Vibration Analysis of Plates by the Superposition Method*, World Scientific, 1999.
- [2] R. Szilard, *Theories and Applications of Plate Analysis: Classical, Numerical and Engineering Methods*, John Wiley & Sons, 2004.
- [3] J.N. Reddy, *Mechanics of Laminated Composite Plates and Shells: Theory and Analysis*, CRC Press, 2004.
- [4] A.W. Leissa, The free vibration of rectangular plates, *Journal of Sound and Vibration*, 31 (1973), 257-293.
- [5] D.J. Gorman, Exact solutions for the free in-plane vibration of rectangular plates with two opposite edges simply supported, *Journal of Sound and Vibration*, 294 (2006), 131-161.
- [6] S.H. Hashemi, M. Arsanjani, Exact characteristic equations for some of classical boundary conditions of vibrating moderately thick rectangular plates, *International Journal of Solids and Structures*, 42 (2005), 819-853.

- [7] Y. Xiang, Y.B. Zhao, G.W. Wei, Lévy solutions for vibration of multi-span rectangular plates, *International Journal of Mechanical Sciences*, 44 (2002), 1195-1218.
- [8] Y. Xiang, G.W. Wei, Exact solutions for vibration of multi-span rectangular Mindlin plates, *Journal of Vibration and Acoustics*, 124 (2002), 545-551.
- [9] Y. Xiang, C.M. Wang, Exact buckling and vibration solutions for stepped rectangular plates, *Journal of Sound and Vibration*, 250 (2002), 503-517.
- [10] Y. Xiang, G.W. Wei, Exact solutions for buckling and vibration of stepped rectangular Mindlin plates, *International Journal of Solids and Structures*, 41 (2004), 279-294.
- [11] S.H. Hashemi, M. Fadaee, H.R.D. Taher, Exact solutions for free flexural vibration of Lévy-type rectangular thick plates via third-order shear deformation theory, *Applied Mathematical Modelling*, 35 (2011), 708-727.
- [12] J.N. Reddy, A.A. Khdeir, L. Librescu, Lévy type solutions for symmetrically laminated rectangular plates using first-order shear deformation theory, *Journal of Applied Mechanics*, 54 (1987), 740-742.
- [13] A.A. Khdeir, J.N. Reddy, L. Librescu, Analytical solution of a refined shear deformation theory for rectangular composite plates, *International Journal of Solids and Structures*, 23 (1987), 1447-1463.
- [14] L. Librescu, A.A. Khdeir, Analysis of symmetric cross-ply laminated elastic plates using a higher-order theory: Part I - Stress and displacement, *Composite Structures*, 9 (1988), 189-213.
- [15] A.A. Khdeir, L. Librescu, Analysis of symmetric cross-ply laminated elastic plates using a higher-order theory: Part II - Buckling and free vibration, *Composite Structures*, 9 (1988), 259-277.
- [16] A.A. Khdeir, Free vibration of antisymmetric angle-ply laminated plates including various boundary conditions, *Journal of Sound and Vibration*, 122 (1988), 377-388.
- [17] A.A. Khdeir, Free vibration and buckling of symmetric cross-ply laminated plates by an exact method, *Journal of Sound and Vibration*, 126 (1988), 447-461.
- [18] J.N. Reddy, A simple higher-order theory for laminated composite plates, *Journal of Applied Mechanics*, 51 (1984), 745-752.
- [19] A.A. Khdeir, J.N. Reddy, Free vibrations of laminated composite plates using second-order shear deformation theory, *Computers and Structures*, 71 (1999), 617-626.
- [20] H.-T. Thai, S.-E. Kim, Lévy-type solution for free vibration analysis of orthotropic plates based on two variable refined plate theory, *Applied Mathematical Modelling*, 36 (2012), 3870-3882.
- [21] E. Carrera, Theories and finite elements for multilayered, anisotropic, composite plates and shells, *Archives of Computational Methods in Engineering*, 9 (2002), 87-140.
- [22] A.K. Noor, W.S. Burton, Assessment of shear deformation theories for multilayered composite plates, *Applied Mechanics Review*, 41 (1989), 1-18.
- [23] J.N. Reddy, D.H. Robbins, Theories and computational models for composite laminates, *Applied Mechanics Review*, 47 (1994) 147-165.
- [24] E. Carrera, Historical review of zig-zag theories for multilayered plates and shells, *Applied Mechanics Review*, 56 (2003), 287-308.
- [25] J.N. Reddy, R.A. Arciniega, Shear deformation plate and shell theories: from Stavsky to present, *Mechanics of Advanced Materials and Structures*, 11 (2004), 535-582.
- [26] C. Wanji, W. Zhen, A selective review on recent development of displacement-based laminated plate theories, *Recent Patents on Mechanical Engineering*, 1 (2008), 29-44.
- [27] M. Boscolo, Analytical solution for free vibration analysis of composite plates with layer-wise displacement assumptions, *Composite Structures*, 100 (2013), 493-510.
- [28] M. Boscolo, J.R. Banerjee, Layer-wise dynamic stiffness solution for free vibration analysis of laminated composite plates,

- Journal of Sound and Vibration*, 333 (2014), 200-227.
- [29] E. Carrera, A class of two dimensional theories for multilayered plates analysis, *Atti Accademia delle Scienze di Torino. Memorie Scienze Fisiche*, 1920 (1995), 49-87.
- [30] L. Dozio, E. Carrera, Ritz analysis of vibrating rectangular and skew multilayered plates based on advanced variable-kinematic models, *Composite Structures*, 94 (2012), 2118-2128.
- [31] E. Carrera, S. Brischetto, Analysis of thickness locking in classical, refined and mixed multilayered plate theories, *Composite Structures*, 82 (2008), 549-562.
- [32] A. Nosier, R.K. Kapania, J.N. Reddy, Free vibration analysis of laminated plates using a layerwise theory, *AIAA Journal*, 31 (1993), 2335-2346.
- [33] J. Hadian, A.H. Nayfeh, Free vibration and buckling of shear-deformable cross-ply laminated plates using the state-space concept, *Computers and Structures*, 48 (1993), 677-693.
- [34] W.Q. Chen, C.F. Lue, 3D free vibration analysis of cross-ply laminated plates with one pair of opposite edges simply supported, *Composite Structures*, 69 (2005), 77-87.

(a) Plate geometry

(b) Example of lamination layout

Figure 1: A rectangular cross-ply laminated plate with one pair of opposite edges simply supported.

(a) Expansion of theory-related indices τ and s

(b) Assembly-like procedure over the layers (example with two layers).

Figure 2: Graphical representation of the expansion and assembly procedure to transform fundamental nuclei of the formulation into the final matrices governing the plate problem.

Figure 3: Combinations of boundary conditions considered in the numerical study.

Table 1: Validation of the present method by comparison with Navier's solutions and 3-D exact analysis for a fully simply-supported square $[0^\circ/90^\circ/0^\circ/90^\circ]$ plate with $b/h = 10$.

(l, m)	Model	Mode					Mode				
		1	2	3	4	5	1	2	3	4	5
(1,1)	3D-exact [32]						0.0662	0.5460	0.6000	1.2425	1.2988
		<i>Navier-type solutions</i>					<i>Present method</i>				
	LD4	0.0662	0.5460	0.6000	1.2425	1.2988	0.0662	0.5460	0.6000	1.2425	1.2988
	LD3	0.0662	0.5460	0.6000	1.2425	1.2988	0.0662	0.5460	0.6000	1.2425	1.2988
	LD2	0.0662	0.5460	0.6000	1.2429	1.2993	0.0662	0.5460	0.6000	1.2429	1.2993
	LD1	0.0665	0.5474	0.6013	1.2762	1.3279	0.0665	0.5474	0.6013	1.2762	1.3279
	ED4	0.0673	0.5480	0.6019	1.2433	1.4109	0.0673	0.5480	0.6019	1.2433	1.4109
	ED3	0.0677	0.5481	0.6020	1.2438	1.4204	0.0677	0.5481	0.6020	1.2438	1.4204
	ED2	0.0689	0.5481	0.6020	1.3716	1.5065	0.0689	0.5481	0.6020	1.3716	1.5065
(2,1)	3D-exact [32]						0.1519	0.6388	1.0761	1.2417	1.3425
		<i>Navier-type solutions</i>					<i>Present method</i>				
	LD4	0.1519	0.6388	1.0761	1.2417	1.3425	0.1519	0.6388	1.0761	1.2417	1.3425
	LD3	0.1519	0.6388	1.0761	1.2417	1.3425	0.1519	0.6388	1.0761	1.2417	1.3425
	LD2	0.1520	0.6388	1.0762	1.2420	1.3430	0.1520	0.6388	1.0762	1.2420	1.3430
	LD1	0.1532	0.6401	1.0877	1.2769	1.3711	0.1532	0.6401	1.0877	1.2769	1.3711
	ED4	0.1571	0.6406	1.0919	1.2433	1.4517	0.1571	0.6406	1.0919	1.2433	1.4517
	ED3	0.1595	0.6407	1.0924	1.2439	1.4611	0.1595	0.6407	1.0924	1.2439	1.4611
	ED2	0.1662	0.6407	1.0931	1.3716	1.5453	0.1662	0.6407	1.0931	1.3716	1.5453

Table 2: Exact dimensionless fundamental frequency $\Omega = (\omega b^2/h)\sqrt{\rho/E_2}$ of a $[0^\circ/90^\circ/0^\circ]$ square plate with various side-to-thickness ratios b/h and different combinations of boundary conditions along x direction.

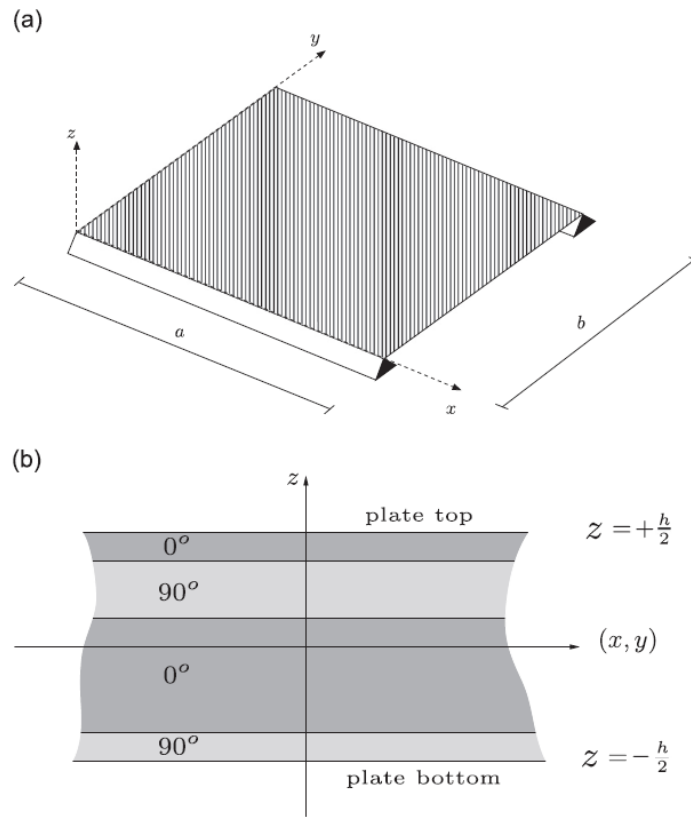
b/h	Model	Boundary conditions					
		SS	SC	CC	FF	FS	FC
	CLPT [33]	18.891	28.498	40.740	4.438	5.076	8.269
50	LD4	18.641	27.484	38.203	4.453	5.078	8.203
	ED3	18.641	27.484	38.203	4.453	5.078	8.203
	TSDT [33]	18.641	27.496	38.231	4.451	5.065	8.216
20	LD4	17.483	23.578	29.993	4.413	5.018	7.973
	ED3	17.488	23.588	30.018	4.423	5.023	7.978
	TSDT [33]	17.483	23.652	30.208	4.422	5.024	7.890
10	LD4	14.696	17.197	19.811	4.289	4.868	7.297
	ED3	14.711	17.226	19.858	4.319	4.893	7.317
	TSDT [33]	14.702	17.427	20.315	4.322	4.895	7.335
5	LD4	10.232	10.749	11.510	3.894	4.408	5.851
	ED3	10.269	10.808	11.593	3.978	4.477	5.911
	TSDT [33]	10.263	11.156	12.333	3.987	4.483	5.975

Table 3: Exact dimensionless fundamental frequency $\Omega = (\omega b^2/h)\sqrt{\rho/E_2}$ of a moderately thick $[0^\circ/90^\circ/0^\circ]$ square plate with various orthotropicity ratios E_1/E_2 and different combinations of boundary conditions along x direction.

E_1/E_2	Model	Boundary conditions					
		SS	SC	CC	FF	FS	FC
2	LD4	6.756	8.221	10.072	2.882	3.706	4.156
	ED3	6.757	8.224	10.081	2.883	3.706	4.156
10	LD4	9.792	12.543	15.507	3.238	3.986	5.136
	ED3	9.794	12.552	15.524	3.239	3.987	5.138
20	LD4	12.054	14.938	17.878	3.634	4.311	6.026
	ED3	12.061	14.954	17.906	3.643	4.317	6.032
	TSDT [17]	12.052	15.036	18.124	3.642	4.313	6.034
	CLPT [17]	13.948	20.610	29.166	3.721	4.443	6.515
30	LD4	13.576	16.293	19.068	3.982	4.602	6.723
	ED3	13.586	16.316	19.106	3.999	4.617	6.736
	TSDT [17]	13.577	16.458	19.448	4.000	4.615	6.744
	CLPT [17]	16.605	24.870	35.431	4.106	4.770	7.445

Table 4: Exact dimensionless fundamental frequency $\Omega = (\omega b^2/h)\sqrt{\rho/E_2}$ for increasing values of m of a $[0^\circ/90^\circ/0^\circ]$ square plate with $b/h = 10$ and different combinations of boundary conditions along x direction.

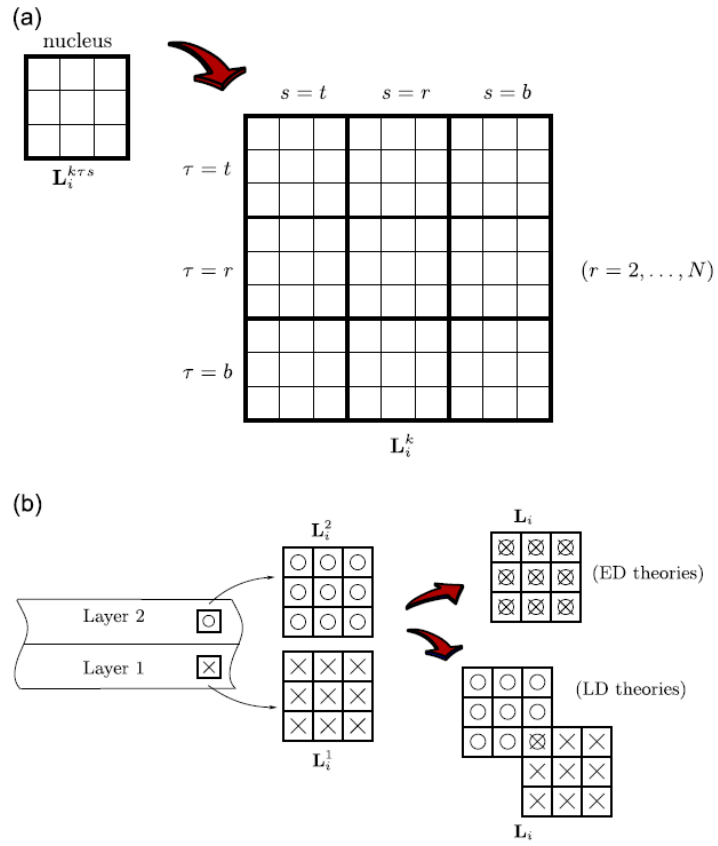
m	Model	Boundary conditions					
		SS	SC	CC	FF	FS	FC
1	3D [34]	14.496	17.195	19.809	–	–	7.256
	LD4	14.696	17.197	19.811	4.289	4.868	7.297
	LD1	14.924	17.583	20.329	4.313	4.891	7.359
	ED4	14.709	17.224	19.854	4.319	4.893	7.317
	ED3	14.711	17.226	19.858	4.319	4.893	7.317
	TSDT [17]	14.702	17.427	20.315	4.322	4.895	7.335
2	3D [34]	21.675	23.289	25.085	–	–	16.998
	LD4	21.676	23.292	25.086	15.576	16.132	16.977
	LD1	21.992	23.718	25.618	15.777	16.331	17.192
	ED4	21.909	23.523	25.321	15.912	16.451	17.282
	ED3	21.911	23.527	25.324	15.913	16.452	17.283
	TSDT [17]	21.914	23.694	25.712	15.948	16.483	17.326
3	3D [34]	34.976	35.877	36.908	–	–	31.929
	LD4	34.976	35.878	36.909	30.992	31.503	31.901
	LD1	35.644	36.609	37.703	31.604	32.111	32.517
	ED4	35.898	36.794	37.821	32.069	32.548	32.936
	ED3	35.913	36.811	37.837	32.082	32.561	32.949
	TSDT [17]	35.982	36.996	38.184	32.203	32.676	33.076
4	LD4	51.541	52.072	52.677	48.557	49.027	49.248
	LD1	52.747	53.316	53.961	49.732	50.196	50.426
	ED4	53.404	53.937	54.546	50.597	51.023	51.242
	ED3	53.461	53.993	54.602	50.649	51.077	51.296
5	LD4	69.751	70.083	70.458	67.326	67.759	67.893
	LD1	71.557	71.916	72.317	69.108	69.536	69.677
	ED4	72.487	72.829	73.217	70.239	70.624	70.761
	ED3	72.629	72.972	73.361	70.378	70.764	70.901



(a) Plate geometry

(b) Example of lamination layout

Figure 1: A rectangular cross-ply laminated plate with one pair of opposite edges simply supported.



(a) Expansion of theory-related indices τ and s

(b) Assembly-like procedure over the layers (example with two layers).

Figure 2: Graphical representation of the expansion and assembly procedure to transform fundamental nuclei of the formulation into the final matrices governing the plate problem.

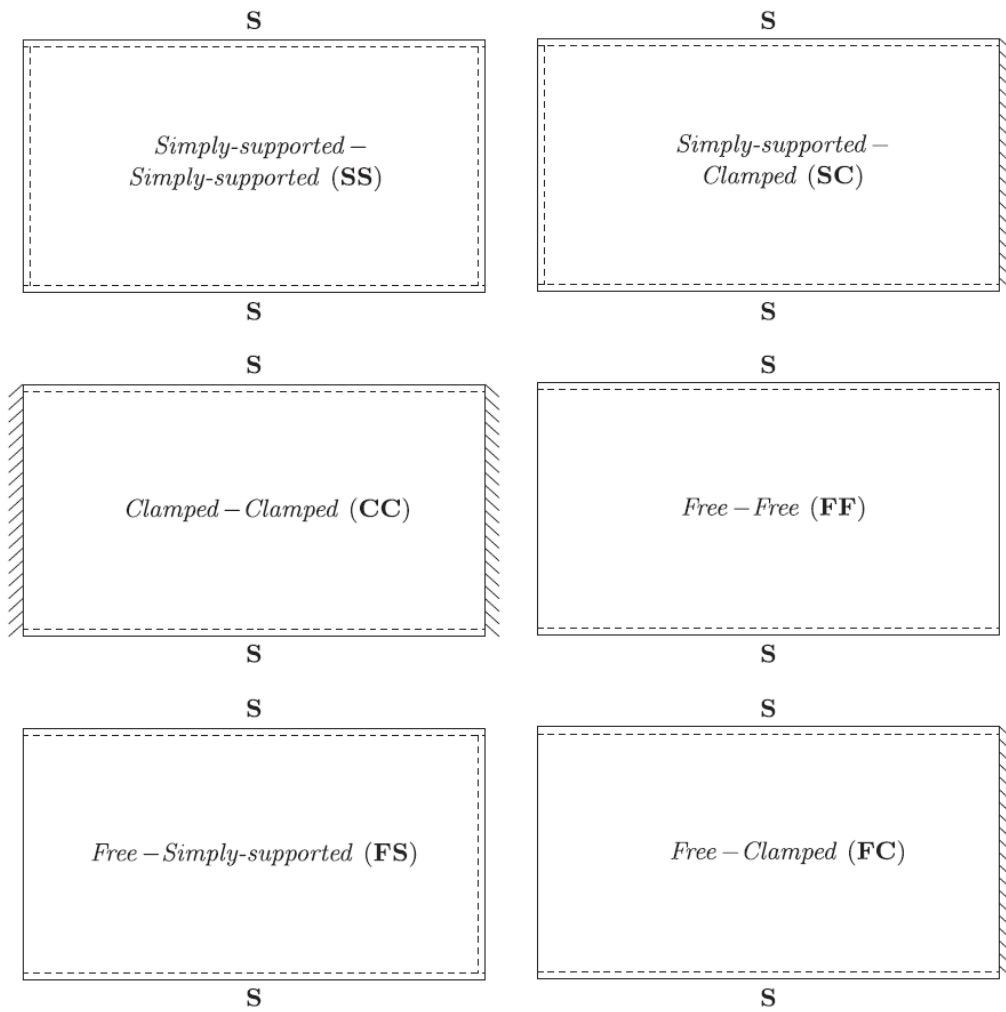


Figure 3: Combinations of boundary conditions considered in the numerical study.